Multi-Purpose Magnetic Particle Analyzer*

A. I. Yavin

I would like to report on some work done by Robert L. Burman and myself. The exact name which I would give this subject is: "Perpendicular Combined Astigmatic Broad-Range Magnetic Spectrograph and Spectrometer." It may be called in short "Astigmatic Enge Magnet" or better still, "Multi-purpose Magnetic Particle Analyzer."

Introduction

A double focusing magnet as a spectrometer was described in 1946 by Svartholm and Siegbahn(1). They showed that if $B(r) \propto (1/r^{1/2})$ in the neighborhood of $r = R$ (where R is the radius of the 360° magnet), a point source of monoenergetic charged particles will come to a focus at an angle $\theta = 2^{1/2}\pi = 254.56°$ in both the radial and axial directions.

Judd(2) discussed the question of two-directional focusing for different field indices n (where $n = -(r/B)(dB/dr)$), and different magnet angles θ.** He treated the case in which both object and image are located outside the magnetic field. The equations which he derived are very useful for any magnet, although only the first order effects were considered in this paper. The equations are:

$$\tan^{-1} n^{1/2} d_o + \tan^{-1} n^{1/2} d_Z + n^{1/2}\theta = \pi \qquad (1)$$

and

$$\tan^{-1} (1-n)^{1/2} d_o + \tan^{-1} (1-n^{1/2} d_r + (1-n)^{1/2} \theta = \pi, \qquad (2)$$

where d_o is the object distance (as measured from the entrance face of the magnet) and d_Z and d_r are the axial and radial image distances, respectively (as measured from the exit face of the magnet). All distances in Judd's paper are in units of R.

$$M_r = [(1-n)^{1/2} d_o \sin (1-n)^{1/2} \theta - \cos (1-n)^{1/2} \theta]^{-1} , \qquad (3)$$

where M_r is the radial magnification. The dispersion D_p is given by

$$D_P = \frac{\delta x}{\delta P/P} = \frac{1 + M_r}{1 - n} \qquad (4)$$

where δx is the normal displacement from the optical axis of an image point of particles with momentum P + δP. The resolution Q can be expressed as

$$Q = \frac{P}{\delta P} = \frac{D_P}{S'} = \frac{D_P}{\alpha M_r S} = \frac{1 + M_r}{\alpha M_r S(1-n)} ,$$

*Supported in part by the Office of Naval Research.

**Note that in the Svartholm Siegbahn case $n = 1/2$ and $\theta = 360°$.

where S' is the collector slit width, α is a number somewhat greater than unity (the aberration factor), and S is the source width. These five equations are sufficient for calculations of object and image distances, dispersion and resolution, slit sizes for a required resolution, etc. A 180° double-focusing spectrometer utilizing the n = 1/2 principle was constructed at the California Institute of Technology.(3)

Judd and Bludman(4) extended Judd's previous calculations to include aberration and fringing effects by expanding the field in the power series given by

$$B_z(r)\Big|_{z=0} = B_o\left[1 - \frac{1}{2}\rho + (\beta_o + \beta_1 a + \beta_2 a^2 + \ldots)\rho^2 + (\gamma_o + \gamma_1 a + \ldots)\rho^3 + \ldots\right], \tag{6}$$

where $\rho = (r-R/R)$, $B_o = (P_o/eR)$, and a is the distance along the optical axis over which the fringing field decreases by an order of magnitude (about one magnet-gap length). The machining of a magnet to take care of these second and third order effects is difficult due to the complex field configuration required. A magnet of this type which has been constructed by Asaro and Perlman at the Lawrence Radiation Laboratory of the University of California has an energy resolution of 0.1% for a solid angle of 0.009 steradians.

Double focusing can be achieved by a uniform-field magnet by either utilizing fringing field effects or by using a quadrupole magnet. The first method was discussed by Cross(5) who showed that axial focusing is achieved in the regions of the fringing field provided the particles enter and leave the magnet at an angle ε (between the path of the particle and the face of the magnet) different from 90°. The magnet angle θ should be small so that the particles will spend an appreciable amount of time in the fringing field (relative to the time they spend in the main field). This requirement causes the object and image distances to be large and, therefore, impractical for small experimental rooms. An additional disadvantage is that the solid angle becomes smaller as the magnet angle θ is decreased.

Browne and Buechner(6) suggested a broad range magnetic spectrograph. Their spectrograph has a uniform magnetic field with a circular boundary of radius R. The source is placed at a distance R from the edge of the field. Particles with energy E will be deflected 90° and will focus radially at a distance R from the exit face of the magnet. Other particles with $0.5E_o \leq E \leq 1.2E_o$ will focus on a hyperbolic surface with the origin being at the center of the circle defined by the boundary of the field.

Enge(7) suggested a combined magnetic spectrograph and spectrometer. He added a quadrupole magnet to the Browne-Buechner spectrograph, resulting in axial focussing with an axial image distance which could be adjusted to the now slightly changed radial image distance. When the quadrupole magnet is turned off, the main magnet can be used as a broad range spectrograph. With the quadrupole magnet on, the range of energies is narrowed but the intensity of each energy component increases so that the combination of the two magnets (hereafter referred to as a spectrometer) becomes more suitable for electronic counting techniques. Enge suggested that the main magnet be placed with its median plane perpendicular to the scattering plane when it is used as a spectrograph, and with its median plane parallel to the scattering plane when it is used as a spectrometer. We shall refer to the former position as the "perpendicular position" and the latter one as the "parallel position."

Mileikowsky(8) suggested an astigmatic magnet with $n \neq 0.5$ and therefore $d_z \neq d_r$, in order to avoid kinematic broadening of the image point. This kinematic broadening is caused by the motion of the recoil nucleus in combination with the finite size of the angular aperture of the entrance to the magnet. It can be shown that when light elements are used as targets, the kinematic energy spread for a scattering-angle aperture of 1^o can be one order of magnitude greater than the resolution. Enge(7) showed that the kinematic broadening could be eliminated to a first order by rotating the Browne-Buechner spectrograph to the parallel position and turning the quadrupole magnet on.

A suggestion is made in this paper to apply Mileikowsky's idea of an astigmatic magnet to Enge's spectrometer. The magnet used in Enge's spectrometer should be kept in the perpendicular position when used both as a spectrograph and as a spectrometer. The current in the quadrupole magnet can now be adjusted to yield any value of $dz - d_r$. It will be possible to cover the continuous region from complete astigmatism ($d_z = \infty$) and therefore small effective solid angle to no astigmatism ($d_z = d_r$) and therefore large effective solid angle. The relative ease of the continuous adjustment of $d_z - d_r$ is very advantageous and should be compared with the difficulty of adjusting n, which in effect means adjusting $d_z - d_r$, in the Mileikowsky case.

Kinematic Broadening

The Q-value equation for the reaction in which particle 1 is impinging on a target nucleus 2 and particle 3 is scattered leaving a residual nucleus 4 is(9)

$$Q = E_3\left(1 + \frac{m_3}{m_4}\right) - E_1\left(1 - \frac{m_1}{m_4}\right) - \frac{2}{m_4}\,(E_1E_3m_1m_3)^{1/2}\cos\theta\,, \tag{7}$$

where θ is the laboratory scattering angle. When Eq. (7) is differentiated with respect to θ, and the terms are rearranged, the result expressed in percent energy change per degree is

$$\frac{1}{E_3}\frac{\partial E_3}{\partial\theta} = -\frac{2(m_1m_3E_1/E_3)^{1/2}\sin\theta}{m_3+m_4-(m_1m_3E_1/E_3)^{1/2}\cos\theta}\cdot\frac{100\pi}{180} \tag{8}$$

For the elastic scattering of alpha particles from C^{12} at scattering angle 90^o Eq. (8) yields

$$\frac{\Delta E_3/E_3}{\Delta\theta} \simeq 1.2\%\ \text{deg}^{-1}.$$

This kinematic broadening puts a severe limitation on the solid angle (see Fig. 268 a,b).

If now a reaction-particle spectrometer with $B \propto (1/r^n)$ is placed in the perpendicular position, n is made different from 0.5, and the detector plate is placed in the radial image point, the image will be a line in the axial direction. This line will be parallel to the axial (Z) direction when the recoiled nucleus has an infinite mass so that no kinematic broadening exists (see Fig. 268c) whereas for a recoiled nucleus with a finite mass the line will be tilted with respect to the axial direction by an angle ψ (see Fig. 268d). Groups of identical particles which leave the residual nucleus at closely spaced energy levels will still be distinguishable, since the

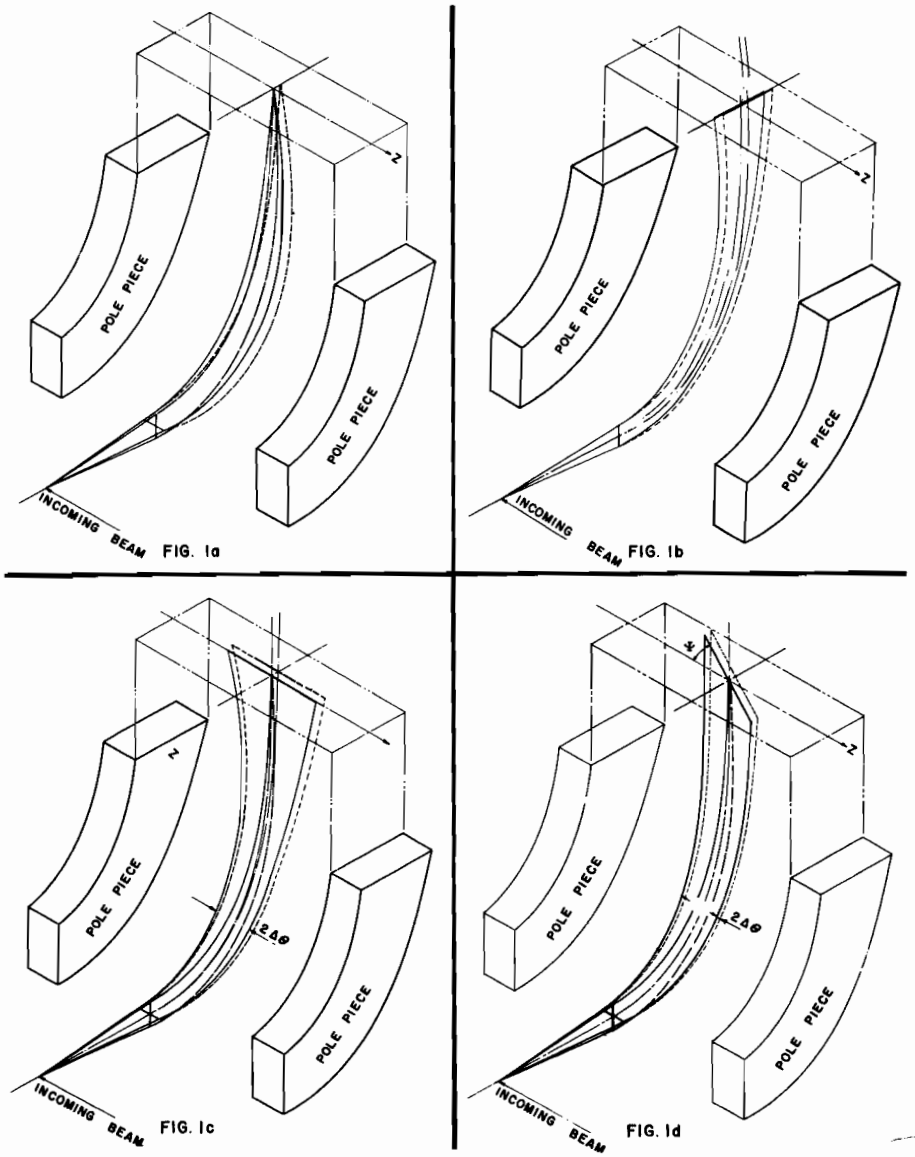

Fig. 268. Astigmatic correction for the kinematic broadening in a 90° defledtion magnet. Spectral images for two energetically-neighboring reaction channels for (a) a stigmatic magnet and a recoil nucleus of infinite mass; (b) a stigmatic magnet and a recoil nucleus of finite mass; (c) an astigmatic magnet and a recoil nucleus of infinite mass; and (d) an astigmatic magnet and a recoil nucleus of finite mass.

kinematic effect is now displaced at the ends of the lines (causing similar tilts to all spectral lines), and the resolving power and solid angle are preserved. In fact, if the n is changed from 0.5 to 0.6, the resolution improves slightly(2). If 2ℓ is the length of the astigmatic image line, then $2\ell \sin \psi$ is the line width due to the kinematic broadening. Mileikowsky suggested that

$$2\ell = 1/2G \tag{9}$$

where G is the gap width. Judd(2) showed that for n near 1/2, the astigmatism for $\theta=\pi$ and $d_o \sim d_z \sim d_r$ is

$$d_z - d_r = 5(1 - 2n)R^* \tag{10}$$

These two relations (o,10) yield

$$n = 1/2\left(1 + \frac{G}{10\ R \tan 2\Delta\theta}\right) , \tag{11}$$

where $2\Delta\theta$ is the acceptance scattering angle. Mileikowsky suggested that the best way of adapting an n = 0.5 magnet to an astigmatic magnet is to insert thin plane sheets of iron between each pole piece and the yoke.

Assuming a unit magnification in both radial and axial directions, and using Eq. (10) the tilting angle can be expressed as

$$\psi = \tan^{-1}\left[-\frac{2}{5}\,\frac{1}{(1-n)(2n-1)}\,\frac{(m_1 m_3 E_1/E_3)^{1/2}\sin\theta}{m_3+m_4-(m_1 m_3 E_1/E_3)^{1/2}\cos\theta}\right] . \tag{12}$$

It is clear from Eq. (12) that ψ depends on the mass m_3 of the scattered particles. This property makes it possible to distinguish between two scattered particles of the same magnetic rigidity, but different masses.

Example 1. Consider 40-Mev alpha particles impinging on a C^{12} target. Let the magnet accept particles at a scattering angle of 90°. The elastically scattered alpha particles will have an energy of 20 Mev. On the other hand, protons from the reaction C^{12} (α, p)N^{15} will have the same magnetic rigidity if the N^{15} is left at a level of excitation ~ 8 Mev. If we choose n = 0.6, the tilting angle for the elastically scattered alpha particles will be

$$\psi_\alpha = \tan^{-1}\left[-\frac{2}{5}\cdot\frac{1}{0.4\ .\ 0.2}\cdot\frac{(4.4.2)^{1/2}}{4+12}\right] = -60.5°$$

The tilting angle for the protons will be

$$\psi_p = \tan^{-1}\left[-\frac{2}{5}\cdot\frac{1}{0.4\ .\ 0.2}\cdot\frac{(4.1.2)^{1/2}}{1+15}\right] = -41.5°$$

Since there is a difference of 19° between the two angles it should be easy to distinguish between the two lines except for the central region where they overlap.

---

*Note that Judd expressed his equations in units of R, so he wrote equation (10) as $d_z - d_r = 5(1 - 2n)$.

It is clear also from Eq. (12) that ψ depends on the mass m_3 of the target nuclei. This property makes it possible to distinguish between identical particles scattered from different isotopes of the same element, or from target contaminations.

Example 2. Consider alpha particles impinging on a natural carbon target. This target consists of nuclides C^{12} and C^{13}, as well as contaminations such as O^{16}, etc.

With n = 0.6, the tilting angles for the elastically scattered alpha particles at 90° are

$$\psi = -60.5° \text{ for } C^{12}(\alpha,\alpha)C^{12} ,$$

$$\psi = -58.3° \text{ for } C^{13}(\alpha,\alpha)C^{13} ,$$

and, $$\psi = -52.2° \text{ for } O^{16}(\alpha,\alpha)O^{16}$$

It is evident that in addition to the difference in energy between the groups of alpha particles, there is also a slight but still noticeable difference in the tilting angles.

The Browne-Buechner Broad-Range Spectrograph

The Browne-Buechner spectrograph has a uniform magnetic field with a circular boundary of radius R and center at C (see Fig. 269). If a source of monoenergetic particles is placed at a radius R from the edge of the field*, an image will be formed at a distance R* from the exit edge of the field if the radius of curvature (of the central ray) is R. The angle of deflection in this case is 90°. A minimum aberration is possible in such an arrangement for a given angular spread at the source(10). Moreover, the circular boundary provides for a normal entrance and exit for the central ray of any other monoenergetic group of particles differing in energy by 50% (or even 100%) from the energy of the first group. The various groups will have different radii of curvature for the central rays, but each group can simultaneously come to a focal point. These focal points lie on a well defined (hyperbolic) focal surface. This magnet is called a broad-range spectrograph since it provides for a simultaneous recording of a broad range of energies.

Radial Focusing. By using the first-order focusing theory of Barber we can easily derive the radial focusing properties of the Browne-Buechner type of magnet. The geometry of the problem is illustrated in Figure 270. The object and image distances (as measured from the faces of the magnet) are d_o and d_r, respectively, and the radius of curvature of the particle in the magnetic field is r. Our derivation follows that in the article(6) by Browne and Buechner.

Since the triangles EBC and EDC are congruent, the angle /EDC is a right angle. Hence the beam enters and leaves normal to the boundary of the magnetic field, and we can use the first order theory of Barber's rule to locate the image point F. As shown in Figure 270, we construct the line through $\overline{AE}$ to intersect the line through $\overline{CD}$ at the point F. Using the x-y axes shown, we find the position of the focal point as a function of r as follows:

*The distance from the face of the pole piece should be R + 2G, since the effective radius (including the effect of the fringing field) is R + G.

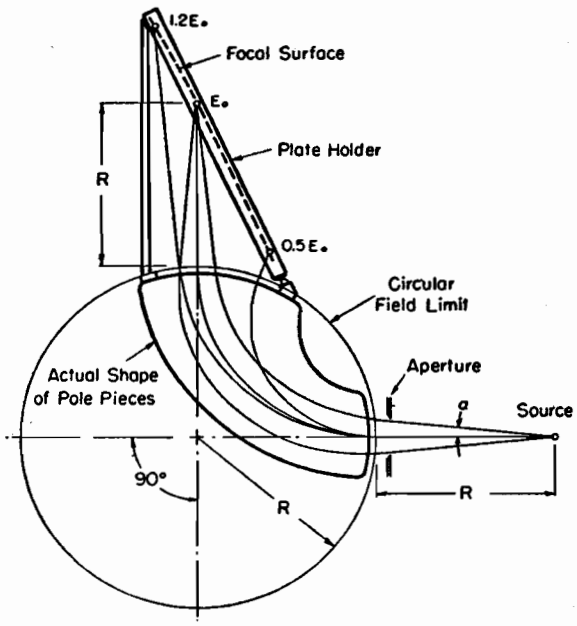

Fig. 269. Schematic drawing of of spectrograph.

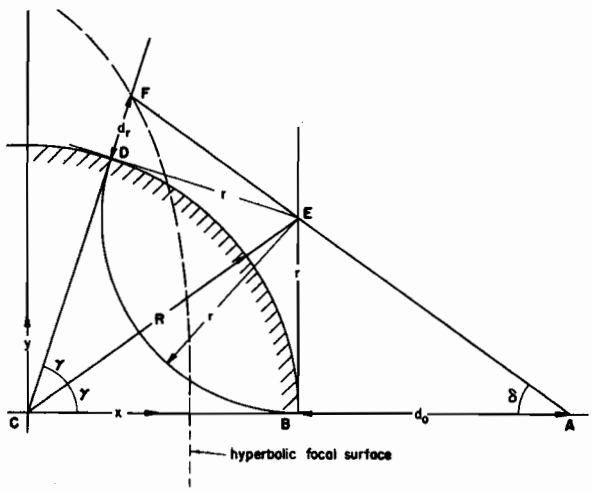

Fig. 270. Drawing for focus theory calculations.

$$x = \overline{CF} \cos 2\gamma$$

$$y = \overline{CF} \sin 2\gamma,$$

and

$$\overline{CF}/\sin\delta = (R+d_o)/\sin(\pi-2\gamma-\delta)$$

$$= (R+d_o)/(\sin2\gamma\cos\delta + \cos2\gamma\sin\delta);$$

thus

$$\overline{CF} = (R+d_o)/(\sin2\gamma\cot\delta + \cos2\gamma).$$

As a function of the radius of curvature, we have

$$\sin\gamma = r/\sqrt{r^2 + R^2},$$

$$\cos\gamma = R/\sqrt{r^2 + R^2}, \text{ and } \cot\delta = d_o/r,$$

so that

$$\overline{CF} = (R+d_o)(R^2+r^2)/(2d_oR + R^2 - r^2). \tag{13}$$

Thus we get

$$\begin{cases} x = (R+d_o)(R^2-r^2)/(2d_oR + R^2 - r^2) \\ y = (R+d_o)(2rR)/(2d_oR + R^2 - r^2) \end{cases}$$

Focal Surface. If we write the solution for the focal point as

$$\begin{cases} x = H(R^2-r^2)/(G-r^2) \\ y = H2rR/(G-r^2), \end{cases} \tag{14}$$

where $H = R + d_o$ and $G = 2d_oR + R^2$, we can eliminate r to get

$$[x-H(G+R^2)/2G]^2 - y(H-R)^2/G = H^2(G+R^2)^2/4G^2 - H^2R^2/G, \tag{15}$$

which gives the focal surface as a hyperbola. For the special case $d_o = R$ (the condition under which the Browne-Buechner magnet is usually operated) we have the focal line

$$(x-4R/3)^2 - y^2/3 = 4R^2/9 . \tag{16}$$

This hyperbola has its center at (4R/3,0) and the focal point at the origin C. The asymptotic slopes are $\pm\sqrt{3}$, so that, if we define the useful range of r by the requirement that the focal point be a finite distance outside the magnet, we want $x^2 + y^2 > R$ and $2\gamma > \tan^{-1} -\sqrt{3}$, or $R/\sqrt{3} < r < \sqrt{3}\,R$.

If we define E_o to be the energy corresponding to r = R, the magnet will simultaneously focus particles with energies from $E_o/3$ to 3 E_o along the hyperbolic focal surface, Eq. (16). The effect of the fringing field will, in general, further restrict the usable energy range. A practical range is $0.5\ E_o \leq E \leq 1.2\ E_o$.

Dispersion. We define the dispersion as (E/R) (ds/dE), where s is the arc length along the hyperbolic focal line. Since $E \propto r^2$ we use E (d/dE) = (r/2) (d/dr) and find

$$\frac{E}{R}\frac{ds}{dE} = \frac{r}{2R}\frac{ds}{dr} = \frac{r}{2R}\sqrt{\left(\frac{dx}{dr}\right)^2 + \left(\frac{dy}{dr}\right)^2} \tag{17}$$

where

$$\frac{dx}{dr} = -\frac{4(R+d_o)r d_o R}{(2d_oR+R^2-r^2)^2}$$

$$\frac{dy}{dr} = \frac{2(R+d_o)(2d_oR^2+r^2R+R^3)}{(2d_oR+R^2-r^2)^2} ,$$

so that we have the dispersion D as

$$D = \frac{E}{R}\frac{ds}{dE} = \frac{r(R+d_o)}{(2d_oR+R^2-r^2)^2}\sqrt{4d_o(d_or^2+d_oR^2+r^2R+R^3) + (R^2+r^2)^2} \tag{18}$$

Again, specializing to the case $d_o = R$,

$$D = \frac{E}{R}\frac{ds}{dE} = \frac{2rR}{(3R^2-r^2)^2}\sqrt{9R^4+10R^2r^2+r^4} \tag{19}$$

Magnification. Using Figure 271 we shall calculate the magnification M_s defined as $\Delta s/\Delta h$, where Δs is the shift along the focal line caused by a lateral displacement Δh of the source. We then have

$$\Delta h = (R+d_o).\Delta\gamma \quad \text{and} \quad \Delta s = (R+d_r)\Delta\gamma/\sin\beta,$$

so that

$$M_s = (R+d_r)/(R+d_o)\sin\beta. \tag{20}$$

here,

$$\beta + 2\gamma = \tan^{-1}\left(\frac{dy}{dx}\right),$$

so that

$$\sin\beta = \sin 2\gamma/\sqrt{1+\left(\frac{dy}{dx}\right)^2} - \frac{dy}{dx}\cos 2\gamma/\sqrt{1+\left(\frac{dy}{dx}\right)^2} . \tag{21}$$

Then, using Eq. (17) and (13), we find

$$M_s = \left(\frac{R+d_r}{R+d_o}\right)\frac{2R}{r}\left(\frac{E}{R}\frac{ds}{dE}\right) / \left(\frac{dy}{dr}\cos 2\gamma - \frac{dx}{dr}\sin 2\gamma\right)$$

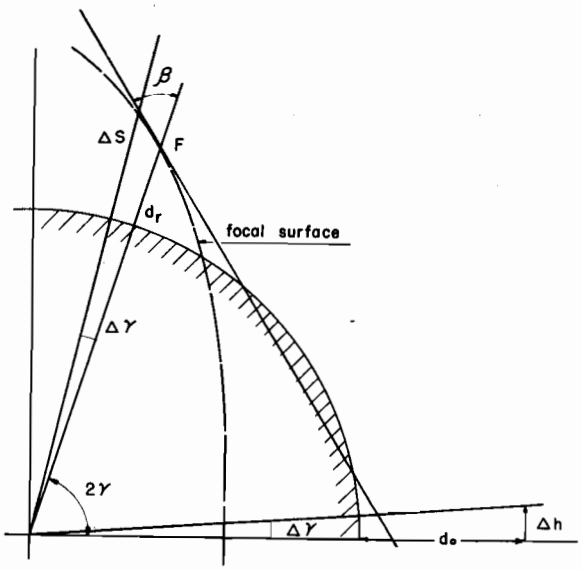

Fig. 271. Drawing for magnification calculations.

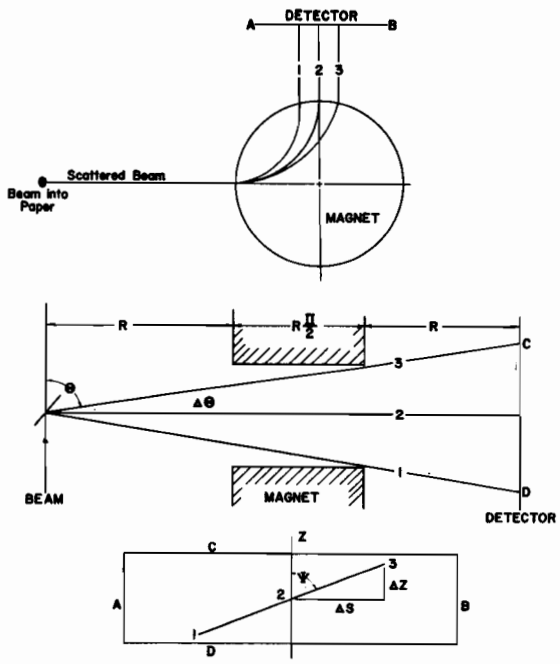

Fig. 272. Line tilting for the Browne-Buechner magnet.

or, (22)

$$M_s = \frac{R^2+r^2}{r(R+d_o)} \left(\frac{E}{R}\frac{ds}{dE}\right) = \frac{R^2+r^2}{r(R+d_o)} D.$$

Aberration. For $d_o = r = R$ (90° deflection) the particle paths are symmetrical about the central rays The focusing condition is then good to second order, and the aberration will depend on α^3, there α is the half-angle of acceptance shown in Figure 269. At deflection angles other than 90° the aberration will be proportional to α^2*. Measurements of the aberration given by Browne and Buechner(6) agree with these predictions. They further indicate that it is not the aberration which limits the resolution, but rather source size, target thickness, initial beam energy resolution, etc.

Line Tilting. We would expect a point source to form a line image, since the n = 0 magnet has no axial focusing. As shown above, the line image will be tilted at an angle ψ; the situation for the Browne-Buechner magnet is shown in Figure 272. Particle number 1, which emerges at an angle larger than θ, has a lower energy in the laboratory than the normal particle, number 2, which emerges at the angle θ, while particle number 3 has a larger energy than number 2. The "tilting angle" is then given by

$$\tan \psi = \frac{\Delta s}{\Delta z}$$

where Δs can be found from the dispersion formula, Eq. (19), with the energy shift ΔE given by Eq. (8). Since there is no axial focusing, we have

$$\Delta z = (2 + \frac{\pi}{2}) R \Delta\theta .$$

*Since the coefficient is much larger than α, the aberration at 90° is much smaller than the aberration at any other deflection angle.

Then with "D" defined as the dispersion,

$$\tan \psi = \frac{\Delta s}{\Delta z} = \frac{DR \frac{\Delta E_3}{E_3}}{(2 + \frac{\pi}{2})R\Delta\theta} = \frac{DR \frac{1}{E_3} \frac{E_3}{\theta} \Delta\theta}{(2 + \frac{\pi}{2})R\Delta\theta} = \frac{2D \frac{1}{E_3} \frac{E_3}{\theta}}{4 + \pi}$$

or

$$\psi = \tan^{-1} \left[- \frac{4D}{(4+\pi)} \frac{\sqrt{m_1 m_3 E_1/E_3 \sin\theta}}{m_3 + m_4 - \sqrt{m_1 m_3 E_1/E_3 \cos\theta}} \right] \quad (23)$$

Solid Angle. Using $\Delta\theta$ as the half angle of acceptance (in degrees) of the scattered beam in the scattering plane, and α as the half-angle (in degrees) in the vertical plane, the solid angle subtended by the magnet is

$$\omega \cong 4\, \alpha\Delta\theta \left(\frac{\pi}{180}\right)^2 \text{ steradians.} \quad (24)$$

The angle $\Delta\theta$ is limited by the gap width of the magnet. For G equal to the gap width,

$$\omega_G = 2\alpha \cdot \frac{\pi}{180} \cdot \frac{G}{(1 + \frac{\pi}{2})R} \cong 1.36 \times 10^{-2}\, \alpha \frac{G}{R} \text{ steradians.} \quad (25)$$

The angle α is essentially limited by effects of the fringing field to be less than 2.5°. The solid angle subtended at the detector will be further reduced by the width W (in the axial direction) of the sensitive surface.

$$\omega_W = 2\alpha \cdot \frac{\pi}{180} \cdot \frac{W}{(2 + \frac{\pi}{2})R} = 9.75 \times 10^{-3}\, \alpha \frac{W}{R} \text{ steradians.} \quad (26)$$

The Combined Magnetic Spectrograph and Spectrometer

The combined magnetic spectrograph and spectrometer which was suggested by Enge(7) is a combination of a Browne-Buechner spectrograph and a quadrupole magnet. The quadrupole magnet, which precedes the spectrograph, provides the axial focusing which is missing in the regular Browne-Buechner magnet, and so converts the spectrograph into a double focusing spectrometer (see Fig. 273). Most of the features (such as resolution, small aberration, etc.) are preserved to a great extent, especially at an angle of deflection 90°, whereas the solid angle is increased. Enge indicates that when the spectrometer is turned into the parallel position, the kinematic broadening can be mostly eliminated.

We would like to suggest that it is more advantageous to keep the magnet in the perpendicular position when the magnet is used both as a spectrograph and a spectrometer. The reasons are two: (1) the acceptance angle 2α in the medium plane of the magnet is geometrically larger than the acceptance angle 2β in the other plane (the plane parallel to the direction of the field). In angular distribution work, the acceptance scattering angle $2\Delta\theta$ should be as small as possible in order to preserve the structure of the distribution. For this reason it is advantageous to have $2\Delta\theta = 2\beta$, and the spectrometer in the perpendicular position. (2) The cost of rotating the

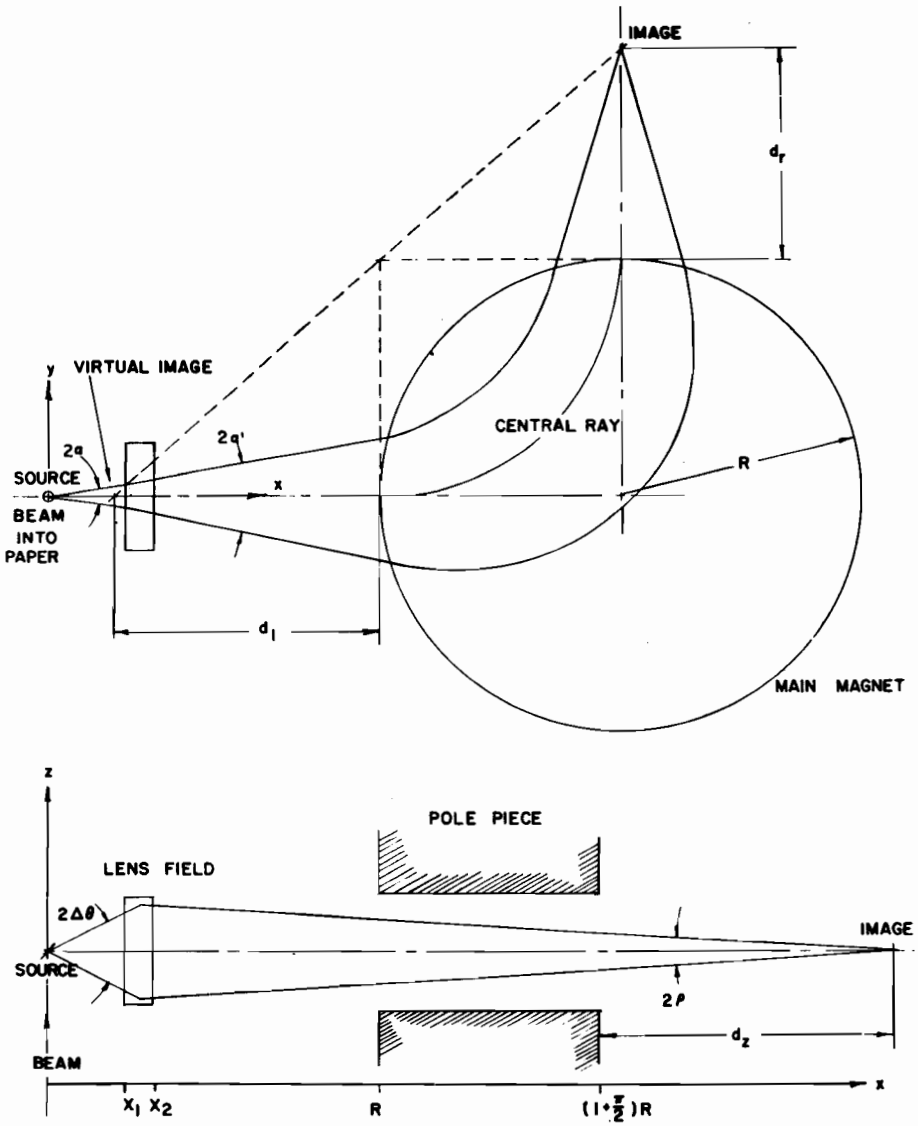

Fig. 273. Quadrupole lens and broad-range spectrograph magnet combined to form double-focusing spectrometer.

magnet from the perpendicular position when used as a spectrograph*, to the parallel position, when used as a spectrometer, is great. The kinematic broadening, on the other hand, can be eliminated by the use of Mileikowsky's idea.

Quadrupole Lens. The radial focusing properties of the Browne-Buechner magnet are modified by the quadrupole lens only in that a virtual object, at a distance d_1 from the cylindrical field boundary, serves as the source for the main magnet. The quadrupole lens is assumed to provide the entire axial focusing for the system.

*It has to be in this position because of the kinematic broadening. It is possible to correct slightly for this broadening by changing the position of the detector plates.

Assuming coordinate axes as shown in Figure 273, with the z-axis parallel to the magnetic field of the main magnet, the y-axis perpendicular to it, and the x-axis along the "normal" path of the scattered beam, we can calculate the focal properties of the quadrupole lens following Enge's treatment.(7) The magnetic field in the quadrupole lens is

$$B = -\frac{B_1}{a} y, \qquad B = -\frac{B_1}{a} z$$

where B_1 is the field at the pole tips and "a" is the distance from the center line to the pole tips. The equations of motion of a charged particle in the lens are

$$\frac{d^2z}{dx^2} + K^2 z = 0 \quad \text{and} \quad \frac{d^2y}{dx^2} - K^2 y = 0 \tag{27}$$

where we have anticipated the correct convergence. Here

$$K^2 = \frac{B_1}{a} \cdot \frac{1}{Br}$$

where Br is the magnetic rigidity (momentum per unit charge) of the particle. For the 90° deflection in the main magnet, we need $Br = B_o R$ where B_o is the field in the main magnet, and R is the radius of curvature of the boundaries. By applying the boundary condition that the logarithmic derivatives by continuous at the physical limits (x_1 and x_2) of the quadrupole lens, Enge obtains the following relationships:

$$d_z = x_2 - \frac{1}{K} \tan K(x_2 - \lambda_1) - R(1 + \frac{\pi}{2}) \tag{28}$$

$$d_1 = R - x_2 + \frac{1}{K} \coth K(x_2 - \lambda_2) \tag{29}$$

$$\begin{cases} \lambda_1 = x_1 - \frac{1}{K} \tan^{-1} (Kx_1) \\ \lambda_2 = x_1 - \frac{1}{K} \coth^{-1} (Kx_1) , \end{cases} \tag{30}$$

where d_z is the distance to the axial image (the image formed by the quadrupole lens) and d_1 is the distance from the virtual image of the quadrupole magnet to the Browne-Buechner magnet. Equation (28) holds exactly for r = R (90° deflection); for the general case, the term $R(1 + \pi/2)$ should be replaced by $R(1 + \pi - 2 \sin^{-1}(r/\sqrt{R^2 + r^2}))$.

These relationships may be kept constant for different energy particles by making $K^2 = B_1/aRB_o$ a constant. This is most easily done by running the two magnets in series. Enge points out that the requirements that the hysteresis loops of the magnets track together limits the ratio of B_1 to B_o to about $B_1/B_o \leq 0.6$ to 0.7.

Radial Focusing. Using the distance d_1 from Eq. (21) in place of d_o, the radial focal surface is again a hyperbola as given by Eq. (15). In particular, for a 90° deflection we have the focal point given by Eq. (14) as

$$x = 0 , \qquad y = R + \frac{R^2}{d_1} , \tag{31}$$

so that the radial image distance from the magnet is

$$d_r = R^2/d_1. \tag{32}$$

Dispersion. The dispersion is given by Eq. (18) with d_o replaced by d_1. For 90° deflection,

$$D_s = \frac{E}{R}\frac{ds}{dE} = \frac{(R + d_1)}{2d_1^2}\sqrt{R^2 + 2Rd_1 + 2d_1^2} \tag{33}$$

where D_s is the dispersion along the focal surface. If we want the dispersion along a direction normal to the particle trajectory, we need

$$D_n = D_s \left|\sin \beta\right|$$

where β is shown in Figure 270. From Eq. (21) of the previous section

$$\sin \beta = (dy/dx)\cos 2\gamma / \sqrt{1 + (dy/dx)^2} - \sin 2\gamma / \sqrt{1 + (dy/dx)^2}$$

or, at 90° deflection (r = R), using Eq. (13) and Eq. (17).

$$\left|\sin \beta\right| = \frac{1}{D_s} \cdot \frac{R + d_1}{2d_1}. \tag{34}$$

The dispersion normal to the beam trajectory is then simply

$$D_n = (R + d_1)/2d_1. \tag{35}$$

Magnification. The inverse focal length of the quadrupole lens in the x-y plane is

$$\frac{1}{f_y} = K \sinh K(x_2 - x_1) \tag{36}$$

and the distance from the first principal plane to the entrance face of the lens is

$$P_y = [\cosh K(x_2 - x_1) - 1] \,/\, K \sinh K(x_2 - x_1). \tag{37}$$

Hence, since the object distance to the first focal plane is

$$x_y = x_1 + P_y - f_y \ , \tag{38}$$

we have the quadrupole magnification in the y-direction as

$$M_{Q_y} = -f_y/x_y = 1/\,[x_1 K \sinh K(x_2 - x_1) + \cosh K(x_2 - x_1)] \tag{39}$$

The magnification along the focal surface of the Browne-Buechner magnet (which follows the quadrupole magnet) is given by Eq. (22) with d_o replaced by d_1 and r = R; the product of this and M_{Q_y} yields

$$M_s = \frac{2RD_s/(R + d_1)}{x_1 K \sinh K(x_2 - x_1) + \cosh K(x_2 - x_1)} \tag{40}$$

where D_x is the dispersion, $(E/R)(ds/dE)$. The magnification M_n along a line normal to the particle trajectory at the focal point is

$$M_n = M_x \, |\sin \beta| \ ,$$

where $|\sin \beta|$ is given by Eq. (34), so that

$$M_n = \frac{R/d_1}{x_1 K \sinh K(x_2 - x_1) + \cosh K(x_2 - x_1)} \tag{41}$$

In the x-z plane the second focal length f_z and the principal plane distance P_z are

$$\frac{1}{f_z} = K \sin K(x_2 - x_1)$$

$$P_z = [1 - \cos K(x_2 - x_1)] \ / \ K \sin K(x_2 - x_1). \tag{42}$$

Using the image distance $x_z' = (1 + (\pi/2))\, R + d_z - (x_2 - P_z + f_z)$ we get

$$M_z = \frac{x_z'}{f_z} = [d_z + (1 + \frac{\pi}{2})R - x_2]\, K \sin K(x_2 - x_1) - \cos K(x_2 - x_1) \tag{43}$$

Astigmatism and Line Tilting. The astigmatism, $d_z - d_r$, is found from Eq. (28) and Eq. (32)

$$d_z - d_r = x_2 - \frac{1}{K} \tan K(x_2 - \lambda_1) - R(1 + \frac{\pi}{2}) - \frac{R^2}{d_1} \tag{44}$$

From Eq. (27) and (28) we can find the emergent half angle ρ (see Fig. 273) for a given half angle $\Delta\theta$:

$$\rho = -K x_1 \frac{\cos K(x_2 - \lambda_1)}{\sin K(x_1 - \lambda_1)} \ \Delta\theta \tag{45}$$

where $\tan \rho$ and $\tan \Delta\theta$ were replaced by ρ and $\Delta\theta$, respectively. The tilting angle ψ, is found from

$$\tan\psi = \frac{\Delta s}{\Delta z} = \frac{\Delta\theta R \frac{1}{E_3} (\frac{\partial E_3}{\partial \theta})\, D}{(d_z - d_r)\, \rho}$$

where D is either D_s (equation (33)) or D_n (equation (35)). This leads to

$$\psi_{s,n} = \tan^{-1} \frac{2RD_{s,n}}{(d_z - d_r)} \frac{\sin K(x_1 - \lambda_1)}{K x_2 \cos K(x_2 - \lambda_1)} \cdot \frac{\sqrt{m_1 m_3 E_1/E_3}\, \sin\theta}{m_3 + m_4 - \sqrt{m_1 m_3 E_1/E_3}\, \cos\theta} \tag{46}$$

Solid Angle. The quadrupole lens opening should be approximately equal to the gap width, G, of the main magnet. Since the maximum particle displacement in the y- or z- direction inside the lens is $a/\sqrt{2}$, we want $a \cong G/\sqrt{2}$. Assuming that the quadrupole acceptance angles define the solid angles, we solve Eq. (27) with the bondary conditions

$$\begin{cases} y = a/\sqrt{2} & \text{at } x = x_2 \\ \dfrac{dz}{dx} = 0 & \text{at } z = a/\sqrt{2} \end{cases}$$

to get the maximum solid angle

$$\omega \cong 4 \tan(\Delta\theta) \tan\alpha$$

$$= 4\left[\frac{a}{\sqrt{2}} K \cos K(x_1 - \lambda_1)\right]\left[\frac{a}{\sqrt{2}} K \frac{\sinh K(x_1 - \lambda_2)}{\cosh K(x_2 - \lambda_2)}\right]$$

or

$$\omega = 2a^2K^2\cos K(x_1 - \lambda_1) \frac{\sinh K(x_1 - \lambda_2)}{\cosh K(x_2 - \lambda_2)} \qquad (47)$$

In practice, however, the solid angle will probably be limited by an aperture, with limits of $\Delta\theta \leq 1^o$ and $\alpha' \leq 2.5^o$. The ratio of α' (see Fig. 273) to α is

$$\frac{\alpha'}{\alpha} = \frac{\sinh K(x_2 - \lambda_2)}{\sinh K(x_1 - \lambda_2)} \quad . \qquad (48)$$

Operation. The parameters of the quadrupole lens are a, x_1, x_2 and $K^2 = B_1/aRB_o$. The magnet gap fixes a minimum value for a, while space limitations define x_1. An appropriate x_2 is then selected. Variations of K through the ratio B_1/B_o can then be used to vary the tilting angle $\psi_{s,n}$ and the axial image size $(d_z - d_r)$.

Examples

Spectrograph. Results of sample calculations based on the formulas above for the Browne-Buechner Broad-Range Spectrograph, assuming R = 66 cm, and $d_o = r = R$ are listed:

$$D = \frac{E}{R}\frac{ds}{dE} = \sqrt{5}$$

$$M_s = \sqrt{5}$$

An energy resolution of 1/1000 corresponds, then, to a displacement at the detector of $\Delta s = 1.47$ mm, and a maximum object width of 0.66 mm. Using the data of Example 1, the calculated tilting angle for $C^{12}(\alpha,\alpha)C^{12}$ is $\psi = 23.9^o$, while for the reaction $C^{12}(\alpha,p)N^{15}$ we find $\psi = -12.0^o$. The solid angle of the system with a detector slit of 2 cm and an acceptance angle $\alpha = 2.5^o$, is 7.4×10^{-4} steradians.

Spectrometer. Sample calculations from the formulas of the preceding section, using R = 66 cm, a = 1.1 cm, x_1 = 18 cm, $B_1/B_o = 0.6$, $\Delta\theta = 1^o$ yield values of K = 1/11, x_2 = 24.2 cm, $x_2 - x_1$ = 6.2 cm, d_1 = 54.6 cm, d_r = 79.8 cm, and d_z = 305.2 cm. From this we find

$$D_n = 1.1$$

$$M_n = 0.57$$

$$M_z = 21.1$$

An energy resolution of 1/1000 corresponds to $\Delta s = 0.72$ mm and a maximum object width of 1.27 mm. Using the same data from section II as above, we get $\psi_n = -78^o$

for $C^{12}(\alpha,\alpha)C^{12}$, and $\psi_n = -67^o$ for $C^{12}(\alpha,p)N^{15}$. Using Eq. (24) with $\Delta\theta = 1^o$, $\alpha' = 2.5^o$, and $(\alpha'/\alpha) = 2.1$ we find a solid angle of 1.5×10^{-3} steradians.

Discussion

The spectrometer (whether parallel or perpendicular) has a 2-4 times larger effective solid angle than the spectrograph (for the 90° deflection particles). Other properties, such as dispersion, resolution, etc., do not change much.

The comparison of the perpendicular spectrometer with the parallel spectrometer yields the following features: (1) The parallel spectrometer has a slightly larger effective solid angle due to the fact that in the parallel position the quadrupole magnet focuses in the direction perpendicular to the scattering plane. When the spectrometer is in the perpendicular position, this axial focusing occurs in the scattering plane, so that any resulting increase in the axial acceptance angle tends to average the angular distribution out. It should be noted on the other hand that initially (before turning the quadrupole magnet on) the perpendicular position is more advantageous since in this position the axial acceptance angle (which is the smaller of the two acceptance angles) is in the scattering plane. (2) The perpendicular combined spectrograph-spectrometer is simpler to construct since it does not require a special arrangement for the conversion from a spectrograph to a spectrometer. This simplicity makes it also much cheaper. (3) Both spectrometers can be adjusted to take care of the kinematic broadening.

JUDD: Thanks for the bouquet with respect to this very old paper. I would like to point out that I have recently been informed that a very nice, complete and elegant calculation of high order aberrations for generality has recently been done by some Japanese. Since I heard about this at the New York meeting I haven't had time to go home and look it up, but you might like to.

CHAIRMAN HAVENS: What is the paper?

JUDD: Some Japanese paper. Also there a number of interesting developments along this line. Many of you know that work is being pursued at Stanford in connection with their various triple and double focusing devices. The expert over there is Dr. Carl Brown who has calculated the aberrations in a variety of situations.

SCHMIDT: With respect to the kinematic broadening, George Farwell and David Daniels, of Washington, have suggested that by changing the position in the focus where you collect the particles you can largely compensate.

References

(1) N. Svartholm and K. Siegbahn. Arkiv för Math, Astr, och Fysik 33, no. 21(1946).

(2) D. L. Judd. Rev. Sc. Instr. 21, 213 (1950).

(3) C. W. Snyder, S. Rubin, W. A. Fowler and C. C. Lauritson. Rev. Sci. Instr. 21, 852 (1950).

(4) D. L. Judd and S. A. Bludman. Nucl. Instr. 1, 46 (1957).

(5) W. G. Cross. Rev. Sci. Instr. 22, 717 (1951).

(6) D. P. Browne and W. W. Buechner. Rev. Sci. Instr. 27, 899 (1956)

(7) H. A. Enge. Rev. Sci. Instr. 29, 885 (1958).

(8) C. Mileikowsky. Arkiv för Fys. 7, 57 (1954).

(9) David Halliday, Introductory Nuclear Physics, (Joh Wiley and Sons, Inc., New York, 1950), p. 378.

(10) E. Segre, Experimental Nuclear Physics, (John Wiley and Sons, Inc., New York, 1953), p. 589 (The paper is by K. T. Bainbridge)